

much lower in the absence of O₂ (Figure 1), and ¹⁸O₂-labeling experiments confirmed that the oxygen atom in the formed C₆H₅CHO was derived predominantly (>60%) from O₂ for three of the oxidants employed. Also detected by gas chromatographic analysis as a product of *cis*-stilbene treatment with activated Fe-BLM was *trans*-stilbene. While formed only to a limited extent in the presence of O₂, *trans*-stilbene was the major product with each oxidant under anaerobic conditions (Figure 1).

That benzaldehyde formation was favored under aerobic conditions, while *trans*-stilbene was formed primarily under anaerobic conditions, suggested that these two products might be derived from a single intermediate that partitioned down one of two pathways depending on the presence or absence of O₂. One candidate for this intermediate is the stilbene cation radical, which could react with O₂ to form benzaldehyde via a dioxetane intermediate or, in the absence of O₂, isomerize to the more stable *trans* configuration and undergo reduction to *trans*-stilbene (Figure 2). It is of interest that photoexcited dyes catalyzed similar chemistry from *cis*-stilbene, with the same O₂ dependence.⁷ In contrast, BLM-mediated stilbene epoxidation was O₂ independent and occurred without loss of stereochemistry. The *cis*-epoxide is apparently formed via a completely different reaction pathway, which may more closely resemble the monooxygenase chemistry of cytochrome P-450.^{5b,8}

Three additional experiments provide support for the scheme outlined in Figure 2. First, the finding that the ratio of C₆H₅CHO to *cis*-stilbene oxide formed under aerobic conditions was essentially constant over the time course (5–30 s) of the H₂O₂-supported reaction was consistent with the formation of both from either a single "activated BLM" intermediate or from two different metal-oxygen species which are kinetically indistinguishable on this time scale. The second finding involved the oxidation of *p*-nitro-*cis*-stilbene under aerobic conditions by Fe^{III}.BLM + H₂O₂. Consistent with the scheme outlined in Figure 2, the ratio of (*p*-nitro)benzaldehyde/(*p*-nitro)-*cis*-stilbene oxide formed was 0.95 for *cis*-stilbene and 0.27 for *p*-nitro-*cis*-stilbene, in parallel with the redox potentials for the two olefins (+1.54 V for *cis*-stilbene; +1.71 V for *p*-nitro-*cis*-stilbene).

While the foregoing results are consistent with the scheme in Figure 2, they do not exclude the possible intermediacy of a stilbene radical; this could form by initial H[•] abstraction in analogy with BLM-mediated DNA oxidation.⁹ Accordingly, the oxidation of *cis*-stilbene was carried out in D₂O/CD₃OD to test this possible mechanism. When activated in deuterated solvent with any of the oxidants in Figure 1, Fe^{III}.BLM catalyzed the conversion of *cis*-stilbene to *trans*-stilbene with no detectable (<1%) deuterium incorporation. While this finding does not exclude a radical intermediate,¹⁰ given the reactivity of the stilbene intermediate toward O₂, and the proposals that many cytochrome P-450-catalyzed reactions proceed via initial electron abstraction,^{8b} the data seem most consistent with the model outlined in Figure 2 and constitute a third line of support.

The nature of the metal-oxo species responsible for the products documented here is uncertain. The similarity in results with each of the oxidants employed suggests, however, that the same intermediate or intermediates are being formed with each oxidant. It is clearly of interest to determine whether the electron abstraction pathway suggested for *cis*-stilbene oxidation is applicable

to the Fe-BLM-mediated oxidation of alkenes *in vivo*.¹¹

Acknowledgment. This study was supported at the University of Virginia by P.H.S. Grant CA38544, awarded by the National Cancer Institute.

(11) Ekimoto, H.; Takahashi, K.; Matsuda, A.; Takita, T.; Umezawa, H. *J. Antibiot.* **1985**, *38*, 1077.

Binuclear Platinum(III) Complexes. Preparation, Structure, and $d\sigma \rightarrow d\sigma^*$ Spectrum of [Bu₄N]₂[Pt₂(P₂O₅H₂)₄(CH₃CN)₂]

Chi-Ming Che,^{*1a} Thomas C. W. Mak,^{*1b}
Vincent M. Miskowski,^{*1c} and Harry B. Gray^{*1c}

Department of Chemistry
University of Hong Kong, Hong Kong
Chinese University of Hong Kong
Shatin, New Territories, Hong Kong
Contribution No. 7427, Arthur Amos Noyes Laboratory
California Institute of Technology
Pasadena, California 91125

Received June 9, 1986

An intense $d\sigma \rightarrow d\sigma^*$ absorption system is the electronic spectroscopic signature of a d^7-d^7 binuclear complex containing a metal-metal single bond.^{2,3} Previous theoretical and experimental work has indicated²⁻⁶ that the highest occupied σ orbital may acquire appreciable axial-ligand character, and, at least in the [Pt₂(P₂O₅H₂)₄X₂]ⁿ⁻ (X = axial ligand) series,^{4,5} the absorption band positions depend so strongly on X that it has not been possible to assign a $d\sigma \rightarrow d\sigma^*$ energy to the Pt-Pt bond itself. We have addressed this problem in the latter series by utilizing CH₃CN as the axial ligand, because its very stable $\sigma(N)$ donor orbital should not significantly contaminate the highest occupied $d\sigma$ Pt-Pt level. Thus the structure and the electronic spectrum of [Pt₂(P₂O₅H₂)₄(CH₃CN)₂]²⁻ should serve as benchmarks in attempts to elucidate axial σ interactions in binuclear platinum(III) complexes.

Dropwise addition of H₂O₂ (30%, 2 mL) to an acetonitrile solution of [Bu₄N]₄[Pt₂(P₂O₅H₂)₄] (0.3 g in 50 mL) containing excess PhSSPh (1 g) yielded a bright yellow solution. Upon addition of diethyl ether, a yellow solid precipitated (> 70% yield). Recrystallization of the crude yellow solid by slow diffusion of diethyl ether into acetonitrile solution gave orange prismatic [Bu₄N]₂[Pt₂(P₂O₅H₂)₄(CH₃CN)₂] crystals together with some starting material.

(1) (a) Department of Chemistry, University of Hong Kong. (b) Department of Chemistry, the Chinese University of Hong Kong. (c) Arthur Amos Noyes Laboratory, California Institute of Technology.

(2) (a) Levenson, R. A.; Gray, H. B. *J. Am. Chem. Soc.* **1975**, *97*, 6042. (b) Pöc, A. J.; Jackson, R. A. *Inorg. Chem.* **1978**, *17*, 2330.

(3) (a) Miskowski, V. M.; Schaefer, W. P.; Sadeghi, B.; Santarsiero, B. D.; Gray, H. B. *Inorg. Chem.* **1984**, *23*, 1154. (b) Miskowski, V. M.; Smith, T. P.; Loehr, T. M.; Gray, H. B. *J. Am. Chem. Soc.* **1985**, *107*, 7925.

(4) (a) Che, C.-M.; Butler, L. G.; Grunthaner, P. J.; Gray, H. B. *Inorg. Chem.* **1985**, *24*, 4662. (b) Che, C.-M.; Lee, W. M.; Mak, T. C. W.; Gray, H. B. *J. Am. Chem. Soc.* **1986**, *108*, 4446. (c) Che, C.-M.; Schaefer, W. P.; Gray, H. B.; Dickson, M. K.; Stein, P. B.; Roundhill, D. M. *J. Am. Chem. Soc.* **1982**, *104*, 4253. (d) Che, C.-M.; Mak, T. C. W.; Gray, H. B. *Inorg. Chem.* **1984**, *23*, 4386. (e) Che, C.-M.; Herbstein, F. H.; Schaefer, W. P.; Marsh, R. E.; Gray, H. B. *J. Am. Chem. Soc.* **1983**, *105*, 4604. (f) Alexander, K. A.; Bryan, S. A.; Fronczek, F. R.; Fultz, W. C.; Rheingold, A. L.; Roundhill, D. M.; Stein, P. B.; Watkins, S. F. *Inorg. Chem.* **1985**, *24*, 2803. (g) Hedden, D.; Walkinshaw, M. D.; Roundhill, D. M. *Inorg. Chem.* **1985**, *24*, 3146.

(5) Isci, H.; Mason, W. R. *Inorg. Chem.* **1985**, *24*, 1761.

(6) Bursten, B. E.; Cotton, F. A. *Inorg. Chem.* **1981**, *20*, 3042.

(7) (a) Eriksen, J.; Foote, C. S. *J. Am. Chem. Soc.* **1980**, *102*, 6083. (b) Lewis, F. D.; Petisce, J. R.; Oxman, J. D.; Nepras, M. J. *J. Am. Chem. Soc.* **1985**, *107*, 203.

(8) White, R. E.; Coon, M. J. *Annu. Rev. Biochem.* **1980**, *49*, 315 and references therein. (b) Guengerich, F. P.; Macdonald, T. L. *Acc. Chem. Res.* **1984**, *17*, 9.

(9) (a) Giloni, L.; Takeshita, M.; Johnson, F.; Iden, C.; Grollman, A. P. *J. Biol. Chem.* **1981**, *256*, 8608. (b) Wu, J. C.; Kozarich, J. W.; Stubbe, J. *J. Biol. Chem.* **1983**, *258*, 4694. (c) Wu, J. C.; Kozarich, J. W.; Stubbe, J. *Biochemistry* **1985**, *24*, 7562.

(10) It is possible that the stilbene radical intermediate might collapse with H[•] abstraction from Fe-BLM. However, the observation that the stilbene intermediate reacts with O₂ in solution, and not with the oxygen of the activated Fe-BLM, suggests that it diffuses away from the BLM "active site" before reacting with O₂.

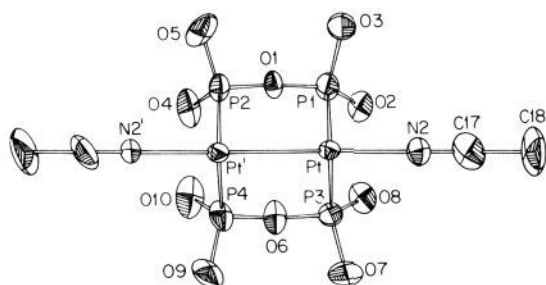


Figure 1. Perspective view of $[\text{Pt}_2(\text{P}_2\text{O}_5\text{H}_2)_4(\text{CH}_3\text{CN})_2]^{2-}$. For clarity, only two bridging pyrophosphites are shown. The primed atoms are related to the unprimed ones by the inversion center at the origin. The thermal ellipsoids are drawn at the 35% probability level.

The structure and atom labeling scheme of the binuclear platinum(III) anion are illustrated in Figure 1.⁷ The complex consists of two face-to-face square-planar PtP_4 units linked by four pyrophosphite groups,⁴ with two axial CH_3CN ligands trans to the Pt-Pt bond. The observed Pt-Pt distance of 2.676 (1) Å is shorter than that in any of the structurally characterized $[\text{Pt}_2(\text{P}_2\text{O}_5\text{H}_2)_4\text{X}_2]^{4-}$ complexes.⁴ Comparison of the structures of $[\text{Pt}_2(\text{P}_2\text{O}_5\text{H}_2)_4(\text{CH}_3\text{CN})_2]^{2-}$ and $[\text{Pt}_2(\text{P}_2\text{O}_5\text{H}_2)_4(\text{CH}_3)(\text{I})]^{4-}$ ($d(\text{Pt-Pt}) = 2.782$ (1) Å)^{4d} reveals that the Pt-Pt bond can be varied over 0.1 Å by axial ligation. The mean Pt-P distance of 2.369 Å and P-O-P angle of 125° are similar to those found for $[\text{Pt}_2(\text{P}_2\text{O}_5\text{H}_2)_4\text{Cl}_2]^{4-}$ ^{4c} and $[\text{Pt}_2(\text{P}_2\text{O}_5\text{H}_2)_4(\text{SCN})_2]^{4-}$.^{4b} The Pt-N distance of 2.093 (10) Å is shorter than that found in $[\text{Pt}_2(\text{P}_2\text{O}_5\text{H}_2)_4(\text{NO}_3)_2]^{4-}$ (2.147 Å)^{4b,g} and $[\text{Pt}_2(\text{P}_2\text{O}_5\text{H}_2)_4(\text{Im})_2]^{4-}$ (2.13 Å).^{4b} Interestingly, the coordinated CH_3CN of $[\text{Pt}_2(\text{P}_2\text{O}_5\text{H}_2)_4(\text{CH}_3\text{CN})_2]^{2-}$ is not substitutionally labile, as the conversion of $[\text{Pt}_2(\text{P}_2\text{O}_5\text{H}_2)_4(\text{CH}_3\text{CN})_2]^{2-}$ to $[\text{Pt}_2(\text{P}_2\text{O}_5\text{H}_2)_4\text{Cl}_2]^{4-}$ in 0.1 M HCl takes more than 1 h.

The UV-vis spectrum of $[\text{Pt}_2(\text{P}_2\text{O}_5\text{H}_2)_4(\text{CH}_3\text{CN})_2]^{2-}$ in acetonitrile (or water) solution exhibits an intense band centered at 211 nm (ϵ 46 500) (Figure 2). Owing to the high ionization energy of the lone-pair $\sigma(\text{N})$ orbital of CH_3CN , the highest-occupied σ level of the d^7-d^7 complex should be the bonding combination of $5d_z^2$ Pt orbitals. Thus $[\text{Pt}_2(\text{P}_2\text{O}_5\text{H}_2)_4(\text{CH}_3\text{CN})_2]^{2-}$ contains a relatively localized Pt-Pt($d\sigma$) single bond, and the 211-nm band is attributable to the fully allowed $d\sigma \rightarrow d\sigma^*$ transition.⁸ The relatively high energy of a (Pt-Pt)-localized $d\sigma \rightarrow d\sigma^*$ excitation clearly shows that the lowest $\sigma \rightarrow d\sigma^*$ systems in $[\text{Pt}_2(\text{P}_2\text{O}_5\text{H}_2)_4\text{X}_2]^{4-}$ species possess substantial $\text{X} \rightarrow \text{Pt}$ charge-transfer character and accordingly should be designated as $\sigma(\text{X}) \rightarrow d\sigma^*$ transitions. The observed dependence of the transition wavelength on $\text{X}(\text{Cl} (282) < \text{Br} (305) < \text{SCN} (337) \sim \text{I} (338 \text{ nm}))$ ^{4a} strengthens this interpretation. The intense band at ~ 215 nm

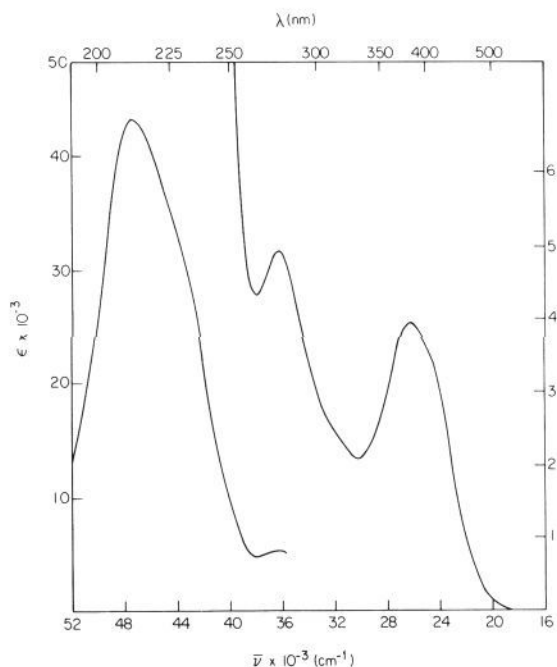


Figure 2. UV-vis absorption spectrum of $[\text{Pt}_2(\text{P}_2\text{O}_5\text{H}_2)_4(\text{CH}_3\text{CN})_2]^{2-}$ in CH_3CN at room temperature.

($\text{X} = \text{Cl}, \text{Br}, \text{I}$)⁵ is logically the $d\sigma \rightarrow d\sigma^*$ transition in these complexes.

Acknowledgment. This research was supported by the Committee of Conference and Research Grants of the University of Hong Kong and National Science Foundation Grant CHE84-19828.

Supplementary Material Available: Tables of atomic coordinates, thermal parameters and selected bond distances and angles (5 pages). Ordering information is given on any current masthead page.

Substrate-Leash Amplification of Ribonuclease Activity

Douglas J. Cecchini, Markus Ehrat,[†] and Roger W. Giese*

Department of Medicinal Chemistry in the College of Pharmacy and Allied Health Professions and Barnett Institute of Chemical Analysis and Materials Science, Northeastern University Boston, Massachusetts 02115

Received May 6, 1986

Chemical amplification takes place when a limited chemical stimulus triggers an enhanced chemical response, as has been reviewed.¹ Here we present a new concept for such amplification, shown in Figure 1. The key feature is that the inactive S-peptide and S-protein fragments of ribonuclease A² (RNase) are immobilized on separate chromatographic gels via a polycytidylic acid (poly C) substrate leash. The addition of free RNase initiates cleavage of this leash. When released S-peptide recombines with the immobilized S-protein, active RNase S forms. The RNase S in turn releases additional enzyme, giving a cascade of enzymatic activity.

[†] Present address: Ciba-Geigy, Basel, Switzerland.

(1) Blaedel, W. J.; Boguslaski, R. C. *Anal. Chem.* **1978**, *50*, 1026-1032.
(2) Richards, F. M.; Wyckoff, H. W. In *The Enzymes*; Boyer, P. D., Ed.; Academic Press: New York, 1971; Vol. IV, pp 647-806.

(7) Crystal data for $[\text{Bu}_4\text{N}][\text{Pt}_2(\text{P}_2\text{O}_5\text{H}_2)_4(\text{CH}_3\text{CN})_2]$: space group, $P2_1/n$, $a = 11.296$ (8) Å, $b = 21.199$ (5) Å, $c = 12.580$ (5) Å, $\beta = 92.46$ (4)°, $z = 2$, $f(000) = 1532$, $d_{\text{measd}} = 1.695$ g cm^{-3} , $d_{\text{calcd}} = 1.691$ g cm^{-3} . A $0.24 \times 0.20 \times 0.16$ -mm crystal was used for data collection. Intensities ($h, k, \pm l$; 5288 unique data) were measured at 22 °C on a Nicolet R3m diffractometer using the ω - 2θ variable-scan 2.02 - 8.37 deg min^{-1} technique in the bisecting mode up to $2\theta_{\text{max}} = 50^\circ$. Azimuthal scans of selected strong reflections over a range of 2θ values were used to define a pseudoellipsoid for the application of absorption corrections ($\mu_r = 0.50$, transmission factors 0.242-0.288). The structure solution was accomplished by means of Patterson and Fourier methods. The binuclear platinum(III) anion occupies a centrosymmetric site in the crystal lattice. All non-hydrogen atoms in the asymmetric unit were varied anisotropically. For the organic cation, the hydrogen atoms were generated geometrically (C-H fixed at 0.96 Å) and included in structure factor calculations with assigned isotropic thermal parameters; the methyl hydrogen atoms were allowed to ride on their respective parent carbon atoms, and the methyl groups were treated as rigid groups. Blocked cascade least-squares refinement converged to $R_F = 0.055$, $R_G = 0.063$, and $S = 1.177$, where $R_F = \sum ||F_o| - |F_c|| / \sum |F_o|$, $R_G = [\sum w(|F_o| - |F_c|)^2 / \sum w|F_o|^2]^{1/2}$ ($w = [\sigma^2(F_o) + 0.0012|F_o|^2]^{-1}$), and $S = [\sum w(|F_o| - |F_c|)^2 / (n - p)]^{1/2}$ ($n = 3713$, number of observed data with $|F_o| > 3\sigma(|F_o|)$, and $p = 328$, number of variables).

(8) The weaker absorption bands at 380, 276, and 232 nm (sh) (Figure 2) are similar both in positions and intensities to features observed in the spectra of other axially ligated d^7-d^7 platinum^{4a} and rhodium⁷ species. The lowest two bands in the spectrum of $[\text{Pt}_2(\text{P}_2\text{O}_5\text{H}_2)_4(\text{CH}_3\text{CN})_2]^{2-}$ are attributable to $d\pi \rightarrow d\sigma^*$ transitions.³